applied sciences

MDPI

Article

A Simple Predator-Prey Population Model with Rich Dynamics

Bing Li [1,2], Shengqiang Liu [1,*], Jing'an Cui [3] and Jia Li [4,*]

1 Academy of Fundamental and Interdisciplinary Science, Harbin Institute of Technology, Harbin 150080, China; leeicer@126.com
2 School of Mathematical Science, Harbin Normal University, Harbin 150025, China
3 College of Science, Beijing University of Civil Engineering and Architecture, Beijing 100044, China; cuijingan@bucea.edu.cn
4 Department of Mathematical Sciences, The University of Alabama in Huntsville, Huntsville, AL 35899, USA
* Correspondence: sqliu@hit.edu.cn (S.L.); li@math.uah.edu (J.L.); Tel.: +86-451-8640-2559 (S.L.); +1-256-824-6470 (J.L.)

Academic Editor: Yang Kuang
Received: 31 March 2016; Accepted: 10 May 2016; Published: 16 May 2016

Abstract: A non-smooth switched harvest on predators is introduced into a simple predator-prey model with logistical growth of the prey and a bilinear functional response. If the density of the predator is below a switched value, the harvesting rate is linear; otherwise, it is constant. The model links the well studied predator-prey model with constant harvesting to that with a proportional harvesting rate. It is shown that when the net reproductive number for the predator is greater than unity, the system is permanent and there may exist multiple positive equilibria due to the effects of the switched harvest, a saddle-node bifurcation, a limit cycle, and the coexistence of a stable equilibrium and a unstable circled inside limit cycle and a stable circled outside limit cycle. When the net reproductive number is less than unity, a backward bifurcation from a positive equilibrium occurs, which implies that the stable predator-extinct equilibrium may coexist with two coexistence equilibria. In this situation, reducing the net reproductive number to less than unity is not enough to enable the predator to go extinct. Numerical simulations are provided to illustrate the theoretical results. It seems that the model possesses new complex dynamics compared to the existing harvesting models.

Keywords: predator-prey model; switched harvest; limit cycle; rich dynamics

MSC: Primary: 92D25, 34K60; Secondary: 34K18

1. Introduction

Mathematical modeling of predator-prey interactions have attracted wide attention since the original work by Lotka and Volterra in 1920s, and there have been extensively studied for their rich dynamics [1–3]. Since the rich and complex dynamics for interactive species are common in the real world, many researchers have investigated the processes that affect the dynamics of prey-predator models and wanted to know what models can best represent species interactions.

As a simplest form, the interaction between a predator and prey may be modeled by a pair of differential equations [1,3–5],

$$\begin{aligned} \frac{dN}{dt} &= rN(1-\frac{N}{K}) - aNP \\ \frac{dP}{dt} &= caNP - dP \end{aligned} \tag{1}$$

where N and P represent the prey and predator species, respectively; r, K, a, c, and d are positive constants. In the absence of the predation, the prey grows logistically with intrinsic growth rate r and carrying capacity K. In the presence of the predator, the prey species decreases at a rate proportional to the functional response aN, where a presents the rate of predation. The factor c denotes the efficiency of predation which divides a maximum per capita birth rate of the predators into a maximum per capita consumption rate. Without the prey, no predation occurs and the predator species decreases exponentially with mortality rate d.

To consider the dynamics of model Equation (1), it is shown that the origin $(0,0)$ is a saddle point. Define the net reproductive number of the predator population n_0, *i.e.*, the expected number of a predator individual producing as the predator population is introduced into a stable prey population [6,7], as

$$n_0 = \frac{caK}{d} \tag{2}$$

Then if $n_0 < 1$, the boundary equilibrium $(K,0)$ with the predator going extinct is globally asymptotically stable and there exists no positive equilibrium for the prey-predator interaction. If $n_0 > 1$, the boundary equilibrium $(K,0)$ is a saddle point and there exists a positive coexistence equilibrium $(N_*, P_*) = \left(\frac{K}{n_0}, \frac{r}{a}\left(1 - \frac{1}{n_0}\right)\right)$, which is globally asymptotically stable. The model dynamics are relatively simple. Using n_0 as bifurcation parameter, we have a transcritical bifurcation at $n_0 = 1$ as (N_*, P_*) is bifurcated. Notice that model Equation (1) is a special case of the prey-predator model in [8].

Apparently, model Equation (1) fails to show the complicated dynamics of the predator-prey interactions in the real world. Later, many researchers improve and enrich model Equation (1) by incorporating some other elements, for example, stage-structure [9–13], nonlinear functional response function [14–18], dispersal among patchers [19], delays [9–11,20], or impulsive effects [18,21].

In the real world, from the point of view of predators' needs, the exploitation of biological resources and harvest are commonly practiced in fishery, forestry, and wildlife management. There is an interest in the use of bioeconomic models to gain insight into the scientific management of renewable resources [16]. Moreover, harvesting is an important and effective method to prevent and control the explosive growth of predators or prey when they are enough. So, generally speaking, it is reasonable and necessary for one to introduce the harvest of populations into models. Taking the above reasons into a consideration, we focus on the predator-prey model with harvest [12,13,16,17,20–28].

Normally, harvesting has several forms in predator-prey models. The most common one of these harvesting forms is a nonzero constant [16,17,20,22–24,26] or a linear harvesting rate [12,13,22,25–28]. In Ref. [22], a two-prey-one-predator model with predator harvested was studied. The authors are particularly interested in the stability properties of different harvest strategies. Two types of harvest strategies are: with a nonzero constant and a linear harvesting rate. The choice of idealized harvest strategies will contribute to a qualitative understanding of the properties of different harvesting strategies. Xiao and Jennings [16] considered the dynamical properties of the ratio-dependent predator-prey model with constant prey harvesting. There existed numerous kinds of bifurcations, such as the saddle-node bifurcation, the subcritical and supercritical Hopf bifurcations. There also existed a limit cycle, a homoclinic or heteroclinic orbit satisfying different parameter values. In Ref. [17], the ratio-dependent predator-prey model with constant predator harvesting was focused on. Philip *et al.* [26] also discussed two predator-prey models with linear or nonzero constant predator harvesting.

The above two types of harvesting rates seemingly have their own advantages as well as disadvantages in fitting the harvest in the real world. When the density of the predator or prey is rather low, the nonzero constant harvesting rate is not as reasonable as of the proportional type [13,22,26]; while if the predator or prey is abundant, linear harvesting rate is less possible than the constant harvesting rate [16]. In Ref. [22], to compare the stability properties of the system

with two harvest strategies, they applied linear or constant harvesting rate, respectively. In that comparative study, the authors demonstrated that switching from linear to constant harvesting rate may turn a stable stationary state to a periodic or chaotic oscillatory mode from a mathematical perspective. However, when deciding the constant level of harvesting, the instability of the constant harvest strategy calls for great care. In Ref. [29], Beddington *et al.* introduced a more realistic smooth harvesting function in which the fishing effort is limited upwards because the constant harvest cannot be achieved for small populations of the fish. The adjustment of a harvesting function can prevent extinction and increase the stability to some extent. Moreover, the dramatic increase of the predator or prey challenges the normal ecological balance and capacity of harvest. Thus, it is interesting to construct a new kind of harvesting rate that combines the advantages from both linear and constant harvesting rates.

Motivated by these ideas, in this paper, we consider a predator-prey model with a novel harvesting rate. Our ideas to develop the harvesting rate are derived from the capacity of treatments of diseases that had been well studied in the dynamical epidemic models [30–32].

Using model Equation (1) as our baseline model, we assume that harvesting takes place, but only the predator population is under harvesting and introduce harvesting function $H(P)$ of the predator to prey-predator model Equation (1) for discussing its dynamical features. The interactive dynamics are governed by the following system

$$\begin{aligned} \frac{dN}{dt} &= rN\left(1-\tfrac{N}{K}\right)-aNP \\ \frac{dP}{dt} &= caNP-dP-H(P) \end{aligned} \tag{3}$$

Following the methods in [14–17,30], we investigate the existence and stability of multiple equilibria, bifurcations, and limit cycles, and study the effects of switched harvest on the dynamics of the predator-prey model.

This paper is organized as follow. Sections 2 and 3.1 represent the boundedness of model Equation (3) and existence of multiple equilibria. In Section 3.2, we study the stability of equilibria, bifurcations, and the existence and stability of a limit cycle. In Section 4, we give numerical simulations to verify our results. Brief discussions are presented finally in Section 5.

2. Model Formulation

Now, we consider model Equation (3). Firstly, we describe harvesting function $H(P)$ of the predators in model Equation (3), which has the following form

$$H(P)=\begin{cases} mP, & 0\le P\le P_0 \\ h, & P_0<P \end{cases} \tag{4}$$

We assume that the harvesting rate is proportional to the predator population size until it reaches a threshold value due to limited facilities of harvesting or resource protection. The harvesting rate will then be kept as a constant. Denote the harvesting threshold value as $h=mP_0$.

When $0\le P\le P_0$, model Equation (3) is

$$\begin{aligned} \frac{dN}{dt} &= rN\left(1-\tfrac{N}{K}\right)-aNP \\ \frac{dP}{dt} &= caNP-dP-mP \end{aligned} \tag{5}$$

When $P > P_0$, model Equation (3) becomes

$$\begin{array}{rcl} \frac{dN}{dt} = & rN\left(1-\frac{N}{K}\right) - aNP \\ \frac{dP}{dt} = & caNP - dP - h \end{array} \tag{6}$$

It is straightforward to verify that solutions of Equation (3) with positive initial conditions are all positive for $t \geq 0$ and ultimately bounded. Thus the following set

$$D = \left\{ (N,P) : N \geq 0, P \geq 0, cN + P \leq \frac{ck(r+d)^2}{4rd} \right\}$$

is positive invariant for system Equation (3).

3. Preliminary Results

3.1. Existence of Equilibria

In this section, we explore the existence of all nonnegative equilibria. First, the origin $(0,0)$ is still a trivial equilibrium and the predator-free equilibrium $(K,0)$ exists. Moreover, it is easy to see that there exists no positive equilibrium in region D if $n_0 \leq 1$. We thus assume $n_0 > 1$ hereafter, and present our results of the existence of positive equilibria as follows.

Theorem 1. *System Equation (3) has a positive coexistence equilibrium $E^*(N^*, P^*)$, in the subregion of D with $0 < P \leq P_0$,*

$$N^* = \frac{K}{\hat{n}}, \quad P^* = \frac{r}{a}\left(1 - \frac{1}{\hat{n}}\right) \tag{7}$$

if and only if $P_0 \geq \frac{r}{a}$ and $\hat{n} > 1$, or $P_0 < \frac{r}{a}$ and $1 < \hat{n} \leq \frac{r}{r - aP_0}$, where $\frac{r}{a}$ represents the maximum predator density for which the prey population can establish itself from a small initial population and $\hat{n}$ is the net reproductive number of the predator under harvesting defined by

$$\hat{n} = \frac{caK}{d+m} \tag{8}$$

Proof. In the subregion of D with $0 < P \leq P_0$, a positive equilibrium of Equation (3) satisfies

$$\begin{cases} rN^*\left(1 - \frac{N^*}{K}\right) - aN^*P^* = 0 \\ caN^*P^* - (d+m)P^* = 0 \end{cases} \tag{9}$$

Then it follows that

$$N^* = \frac{d+m}{ca} = \frac{K}{\hat{n}}$$

and then

$$P^* = \frac{r}{a}\left(1 - \frac{1}{\hat{n}}\right) > 0$$

if $\hat{n} > 1$. In the mean time, it follows from

$$P^* = \frac{r}{a}\left(1 - \frac{1}{\hat{n}}\right) \leq P_0$$

and then

$$\frac{1}{\hat{n}} \geq \frac{r - aP_0}{r}$$

that there exists a positive equilibrium in this subregion if

$$\frac{r - aP_0}{r} \leq 0$$

or if $\frac{r - aP_0}{r} > 0$ and

$$\hat{n} \leq \frac{1}{1 - \frac{aP_0}{r}} = \frac{r}{r - aP_0} \tag{10}$$

□

To investigate the existence of positive equilibria in the subregion of D with $P > P_0$, we first give the relation of roots and coefficients for a quadratic equation.

Quadratic equation $(x - A)(B - x) = C$, with constants A, B, and C positive, has two positive roots

$$x_1 = \frac{A + B - \sqrt{(B - A)^2 - 4C}}{2} < x_2 = \frac{A + B + \sqrt{(A - B)^2 - 4C}}{2}$$

a unique positive root

$$x = \frac{A + B}{2}$$

or no positive root, if

$$C < \frac{(B - A)^2}{4},\ C = \frac{(B - A)^2}{4},\ \text{or}\ C > \frac{(B - A)^2}{4}$$

respectively.

The results for the existence of positive equilibria of Equation (3) in the subregion of D with $P > P_0$ are provided as follows.

Theorem 2. *We assume* $P_0 < \frac{r}{a}$ *and define*

$$\hat{P} = \frac{r(n_0 - 1)}{2an_0},\ h_1 = \frac{crK}{4}\left(1 - \frac{1}{n_0}\right)^2,\ h_2 = \frac{rm}{a}\left(1 - \frac{1}{\hat{n}}\right) \tag{11}$$

System Equation (3)*, in the subregion of D with* $P > P_0$*, has*

(a) No positive equilibrium if

$$h > h_1, \quad or \quad \begin{cases} P_0 > \hat{P} \\ h_2 \leq h < h_1 \end{cases}$$

(b) A unique positive equilibrium with

$$N = \frac{K(1 + n_0)}{2n_0}, \quad P = \frac{r(K - N)}{aK} = \frac{r(n_0 - 1)}{2an_0} \tag{12}$$

if

$$h = h_1, \quad \begin{cases} P_0 > \hat{P}, \\ h < h_1 \text{ and } h < h_2 \end{cases} \quad or \quad \begin{cases} P_0 < \hat{P}, \\ h < h_1 \text{ and } h \leq h_2 \end{cases}$$

(c) Two positive equilibria $E_i(N_i, P_i)$*,* $i = 1, 2$*, where*

$$\begin{aligned} N_1 &= \frac{crK(1 + n_0) - n_0\sqrt{4crK\,(h_1 - h)}}{2crn_0} \\ &< \frac{crK(1 + n_0) + n_0\sqrt{4crK\,(h_1 - h)}}{2crn_0} = N_2 \end{aligned} \tag{13}$$

and

$$P_2 = \frac{r(K-N_2)}{aK} < P_1 = \frac{r(K-N_1)}{aK}$$

if $h < h_1$ *and*

$$\begin{cases} P_0 < \hat{P} \\ \hat{n} < 1 \end{cases} \quad or \quad \begin{cases} P_0 < \hat{P} \\ h_2 < h \end{cases}$$

Proof. In the subregion of D with $P > P_0$, a positive equilibrium satisfies

$$rN(1-\frac{N}{K}) - aNP = 0 \tag{14a}$$

$$caNP - dP - h = 0 \tag{14b}$$

It follows from Equation (14a) that

$$P = \frac{r(K-N)}{aK}$$

Substituting it into Equation (14b) yields

$$\left(N - \frac{K}{n_0}\right)(K-N) = \frac{K}{cr}h \tag{15}$$

It follows from the relation of roots and coefficients for the quadratic equation $(x-A)(B-x) = c$ shown above that equation Equation (15) has no, unique, or two positive solutions if $h > h_1$, $h = h_1$, or $h < h_1$.

To have $P_i > P_0$, $i = 1, 2$, we need

$$P_i = \frac{r(K-N_i)}{aK} > P_0$$

that is,

$$N_i < K - \frac{aK}{r}P_0 = \frac{aK}{r}\left(\frac{r}{a} - P_0\right), \quad i = 1, 2 \tag{16}$$

Thus, if $P_0 \geq r/a$, there is no positive equilibrium of Equation (15) in the subregion of D with $P > P_0$. We assume $P_0 < r/a$.

Suppose there are two positive solutions, $N_1 < N_2$, to Equation (15) and hence $P_2 < P_1$. Then $P_2 > P_0$ if and only if

$$N_2 < K - \frac{aK}{r}P_0 \tag{17}$$

Substituting N_2 in Equation (13) into Equation (17) yields

$$n_0\sqrt{4crK\,(h_1-h)} < crK(n_0-1) - 2caKn_0P_0$$

that is,

$$\frac{\sqrt{4crK}}{2caK}\sqrt{(h_1-h)} < \frac{r(n_0-1)}{2an_0} - P_0 = \hat{P} - P_0 \tag{18}$$

Then if $P_0 \geq \hat{P}$, we have $P_2 \leq P_0$.

Assume $P_0 < \hat{P}$. Squaring both sides of Equation (18) yields

$$\frac{r}{ca^2K}(h_1-h) < \frac{r^2(n_0-1)^2}{4a^2n_0^2} - \frac{r(n_0-1)}{an_0}P_0 + P_0^2 \tag{19}$$

It follows from the definition of h_1 that

$$\frac{rh_1}{ca^2K} = \frac{r}{ca^2K}\frac{crK(n_0-1)^2}{4n_0^2} = \frac{r^2(n_0-1)^2}{4a^2n_0^2}$$

Then Equation (19) becomes

$$\begin{aligned} 0 < h^2 - \frac{rm}{a}\left(\frac{n_0-1}{n_0} - \frac{m}{caK}\right)h &= \left(h - \frac{rm}{a}\left(1 - \frac{d+m}{caK}\right)\right)h \\ &= \left(h - \frac{rm}{a}\left(1 - \frac{1}{\hat{n}}\right)\right)h \end{aligned} \tag{20}$$

If $\hat{n} < 1$, we have $P_2 > P_0$. Otherwise, Equation (20) is equivalent to

$$0 < (h - h_2)h$$

Thus, if $h_2 < h < h_1$, $P_2 > P_0$, and if $h \leq h_2$, $P_2 < P_0$.
We now consider $P_1 > P_0$, that is,

$$N_1 < \frac{aK}{r}\left(\frac{r}{a} - P_0\right) \tag{21}$$

Substituting N_1 in Equation (13) into Equation (21), we have

$$\frac{\sqrt{4crK}}{2caK}\sqrt{(h_1 - h)} > P_0 - \hat{P} \tag{22}$$

If $P_0 \leq \hat{P}$, inequality Equation (21) is satisfied which implies $P_1 > P_0$.
Suppose $P_0 > \hat{P}$. Similarly as above, inequality Equation (22) is equivalent to

$$0 > (h - h_2)h$$

Thus, if $h < h_2$, $P_1 > P_0$, and if $h \geq h_2$, $P_1 < P_0$.
By putting all together, the proof is completed. □

Remark 1. System Equation (1) with linear predator harvest strategy leads to the predator extinct if the net reproductive number $\hat{n} < 1$. However, by Theorem 2 (c), we find that for system Equation (1) with switched predator harvest strategy; that is, when the density of predator is below harvest level P_0, the linear harvesting rate is applied to the system, whereas when the density of predators is higher than harvest level, the system adopts nonzero constant harvesting rate, even if $\hat{n} < 1$, the prey and predator may coexist.

3.2. Stability of Equilibria

In this section, we discuss the stability of equilibria of model Equation (3).

Theorem 3. *Equilibrium $E_0(K,0)$ is locally asymptotically stable if $\hat{n} < 1$, and unstable if $\hat{n} > 1$. Moreover, $E_0(K,0)$ is globally asymptotically stable in $D\backslash\{(0,0)\}$ if $\hat{n} < 1$ and $h > h_1$. If $\hat{n} > 1$, system Equation (3) is permanent.*

Proof. It is easy to obtain that the characteristic roots to the linearized equation of system Equation (3) at $E_0(K,0)$ are $\lambda_1 = -r < 0$ and $\lambda_2 = caK - d - m = (d+m)(\hat{n}-1)$. Thus, E_0 is locally asymptotically stable if $\hat{n} < 1$ and unstable if $\hat{n} > 1$.

Next, note that $(0,0)$ is always unstable. If $\hat{n} < 1$, by Theorems 1 and 2, there is not any other equilibrium of system Equation (3) than E_0 in $D\backslash\{(0,0)\}$. Since D is the invariant set of system

Equation (3) and E_0 is locally asymptotically stable, it follows from the Bendixson Theorem that every solution of system Equation (3) in D approaches E_0 when t tends to positive infinity.

Since E_0 is unstable as $\hat{n} > 1$, following the similar arguments to Cantrell and Cosner ([33] Theorem 3.1) (see also ([34] Theorems 3,4)), which is based on the uniform persistence theory introduced by Hale and Waltman [35], we are able to conclude that system Equation (3) is permanent if $\hat{n} > 1$.

The proof is complete. □

Remark 2. It follows from Cantrell and Cosner ([33] Theorem 3.1) that system Equation (5) is permanent if and only if $\hat{n} > 1$. Thus Theorem 3 suggests that if system Equation (5) is permanent, then so is system Equation (3).

For the three positive equilibria E^*, E_1, E_2, we have the following results. Firstly, we consider the stability of E^*.

Theorem 4. *The positive equilibrium $E^*(N^*, P^*)$ of system Equation (3) is globally asymptotically stable if $P_0 < \frac{r}{a}$ and $1 < \hat{n} \leq \frac{r}{r - aP_0}$.*

Proof. According to Theorem 1, positive equilibrium $E^*(N^*, P^*)$ exists if and only if $P_0 < \frac{r}{a}$ and $1 < \hat{n} \leq \frac{r}{r - aP_0}$. The Jacobian matrix of system Equation (3) at $E^*(N^*, P^*)$ is

$$J^* = \begin{pmatrix} r(1 - \frac{N^*}{K}) + rN^*(-\frac{1}{K}) - aP^* & -aN^* \\ caP^* & caN^* - d - m \end{pmatrix} \tag{23}$$

Because N^* and P^* satisfy Equation (9), by means of Equation (9), the trace and determinant of J^* are simplified as

$$\begin{aligned} tr(J^*) &= r - \frac{2rN^*}{K} - aP^* + caN^* - d - m = -\frac{rN^*}{K} < 0 \\ det(J^*) &= (r - \frac{2rN^*}{K} - aP^*)(caN^* - d - m) + ca^2N^*P^* = ca^2N^*P^* > 0 \end{aligned} \tag{24}$$

Therefore, all eigenvalues of matrix J^* have negative real parts when $P_0 < \frac{r}{a}$ and $1 < \hat{n} \leq \frac{r}{r - aP_0}$. It follows that $E^*(N^*, P^*)$ is locally asymptotically stable.

Then, it suffices for us to prove the global attractiveness of $E^*(N^*, P^*)$. Inspired by the work of McCluskey [36], we define a Lyapunov function

$$M(t) = cN^*(\frac{N(t)}{N^*} - \ln\frac{N(t)}{N^*} - 1) + P^*(\frac{P(t)}{P^*} - \ln\frac{P(t)}{P^*} - 1)$$

where $N^* = \frac{K}{\hat{n}}$, and $P^* = \frac{r}{a}(1 - \frac{1}{\hat{n}})$.

We know that $\frac{N(t)}{N^*} - \ln\frac{N(t)}{N^*} - 1$ and $\frac{P(t)}{P^*} - \ln\frac{P(t)}{P^*} - 1 \geq 0$ for all $N(t), P(t) > 0$. (The equality holds if and only if $N(t) = N^*, P(t) = P^*$.) From the definition of $M(t)$, we know that $M(t)$ is well-defined and $M(t) \geq 0$. The equality holds if and only if $N(t) = N^*$ and $P(t) = P^*$.

Differentiating $M(t)$ along the solutions of system Equation (3), we obtain

$$\begin{aligned}\frac{dM(t)}{dt} &= c(1-\frac{N^*}{N})\frac{dN}{dt}+(1-\frac{P^*}{P})\frac{dP}{dt}.\\ &= -\frac{cr}{K}N^2+\frac{2rN(d+m)}{aK}-\frac{r(d+m)^2}{ca^2K}.\\ &= -\frac{cr}{K}(N-\frac{d+m}{ca})^2\leq 0\end{aligned}$$

It follows that $M(t)$ is bounded and non-increasing. Thus $\lim_{t\to\infty} M(t)$ exists. Note that $\frac{dM}{dt}=0$ if and only if $N=N^*$. Substituting $N=N^*$ into the first equation of Equation (3), one can directly get $P=P^*$. Therefore, the maximal compact invariant set in $\frac{dM}{dt}=0$ is the singleton E^*. By the LaSalle invariance principle (see, for example, Theorem 5.3.1 in Hale and Verduyn Lunel [37]), positive equilibrium E^* is globally attracting. Further, E^* is globally asymptotically stable. □

Now we concentrate on the stability of coexistence equilibria $E_i(N_i,P_i)$, $i=1,2$. The Jacobian matrix of system Equation (3), at $E_i(N_i,P_i)$, is

$$J_i=\begin{pmatrix} r-\frac{2rN_i}{K}-aP_i & -aN_i \\ caP_i & caN_i-d\end{pmatrix},\quad i=1,2 \tag{25}$$

Theorem 5. *If the coexistence equilibrium $E_2(N_2,P_2)$ of system Equation (3) exists, it is unstable.*

Proof. For the coexistence equilibrium $E_2(N_2,P_2)$, N_2 and P_2 satisfy Equation (14). By Equations (13)–(15), after direct calculations, the determinant of matrix J_2 is

$$det(J_2)=-\frac{2car}{K}(N_2-\frac{d+caK}{4ca})^2+\frac{2car(d+caK)^2}{16c^2a^2K} \tag{26}$$

Because

$$N_2=\frac{crK(1+n_0)+n_0\sqrt{4crK(h_1-h)}}{2crn_0}>\frac{crK(1+n_0)}{2crn_0}=\frac{caK+d}{2ca}$$

we obtain that $det(J_2)<0$. Thus $E_2(N_2,P_2)$ is a saddle point and unstable. □

For the coexistence equilibrium $E_1(N_1,P_1)$, similarly, the determinant of J_1 is

$$det(J_1)=-\frac{2car}{K}(N_1-\frac{d+caK}{4ca})^2+\frac{2car(d+caK)^2}{16c^2a^2K} \tag{27}$$

but since

$$N_1=\frac{crK(1+n_0)-n_0\sqrt{4crK(h_1-h)}}{2crn_0}<\frac{crK(1+n_0)}{2crn_0}=\frac{caK+d}{2ca}$$

we obtain $det(J_1)>0$, and $E_1(N_1,P_1)$ may be node, focus or center.

By Equations (13)–(15), the sign of the trace of matrix J_1 is determined by

$$\varphi=r^2d(d-caK)+2ca^2K(caK-r)h-ard\sqrt{4crK(h_1-h)} \tag{28}$$

According to Equation (28), we obtain

(a) If $caK-r\leq 0$, then $\varphi<0$.

(b) If $caK-r>0$, and $h\leq\frac{r^2d(caK-d)}{2ca^2K(caK-r)}=\frac{r^2d^2(n_0-1)}{2ca^2K(caK-r)}=h_3$, then $\varphi<0$.

(c) If $caK-r>0$, $h>h_3$ and $\eta=4crK(h_1-h)-\frac{[2ca^2K(caK-r)h-r^2d^2(n_0-1)]^2}{a^2r^2d^2}>0$, then $\varphi<0$.

Summarizing the above discussions, we have the following results on the stability of equilibrium $E_1(N_1, P_1)$.

Theorem 6. *Suppose that the coexistence equilibrium $E_1(N_1, P_1)$ exists and if one of following conditions is satisfied:*

(a) $caK \leq r$;
(b) $caK > r$ *and* $h \leq h_3$;
(c) $caK > r$ *and* $h > h_3$ *and* $\eta > 0$,

then $E_1(N_1, P_1)$ is locally asymptotically stable. It is unstable if $caK > r, h > h_3$, and $\eta < 0$.

Combining the existence and stability results of equilibria of model Equation (3), by following similar arguments to ([31] Corollary 2.3), we present the following corollary to give conditions for bifurcation.

Corollary 1. *If $\hat{n} < 1$ and $h < min\{h_1, m\hat{P}\}$, then system Equation (3) has a backward bifurcation of positive equilibria.*

Next, we give examples to demonstrate the bifurcation of multiple equilibria.

For various parameter values, model Equation (3) has a forward bifurcation from one positive equilibrium to another positive equilibrium (see Example 3.1.) and a backward bifurcation with a predator-extinct equilibrium and two positive equilibria (Example 3.2.). Note that the conditions in Theorem 2 *a*) and Theorem 2 *c*) guarantee the existence of three positive equilibria E^* and E_1, E_2 (Example 3.3.).

Example 3.1. Using the following parameter values $r = 0.1, K = 0.5, a = 0.25, c = 0.8, d = 0.01$, and $m = 0.03$, we obtain $\hat{n} = 2.5$, and $h_2 = 0.0072$. When $h \leq h_2$, a bifurcation diagram is shown in Figure 1. When the parameter h decreases, the bifurcation at $h = h_2$ is forward, and model Equation (3) has a unique positive equilibrium for $h > 0$, which is similar to ([30] Example 2.4).

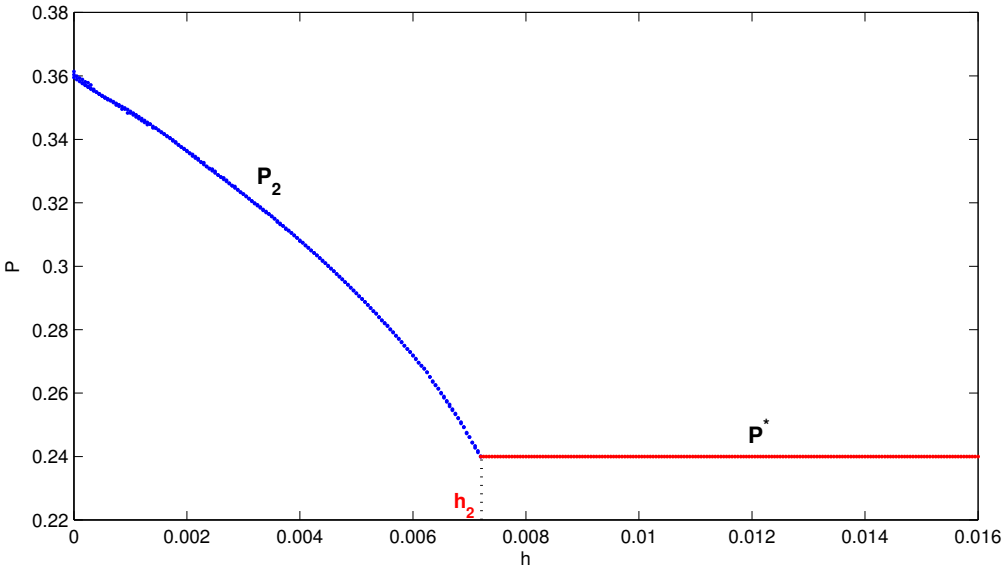

Figure 1. The forward bifurcation diagram from P^* to P_1 *versus* u for Equation (3). The line with P_1 indicates the curve of the predator with coexistent equilibrium E_1, and the line with P^* indicates the curve of the predator with coexistent equilibrium E^*.

Example 3.2. Choosing $r = 0.1, K = 0.4, a = 0.1, c = 0.8, d = 0.01$, and $m = 0.03$, we obtain $\hat{n} = 0.8 < 1$, $h_1 = 0.00378$, and $\hat{P} = 0.34367$. A backward bifurcation diagram is given in Figure 2, where the horizontal line denotes the curve of the predator with predator-extinct equilibrium E_0. Two positive equilibria E_1 and E_2 arise simultaneously at $h = h_1$ when the parameter h decreases.

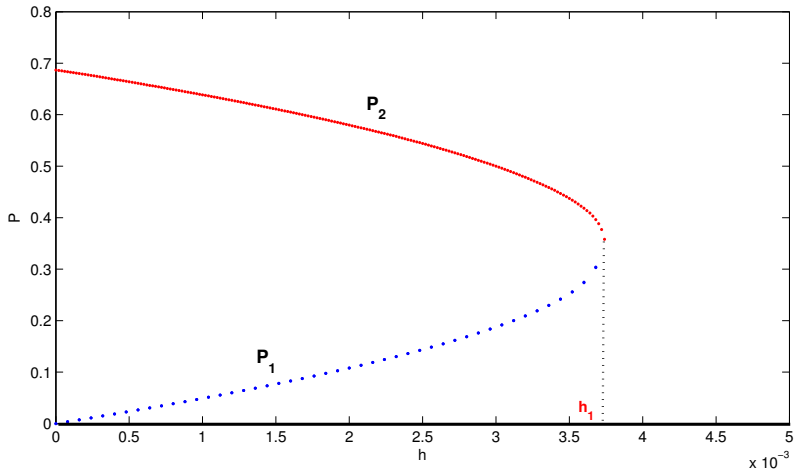

Figure 2. The backward bifurcation diagram of P_1 and P_2 *versus* h for Equation (3). The solid line with P_1 and dotted line with P_2 represent the curves of the predator with coexistent equilibrium E_1 and E_2, respectively.

Remark 3. In Figure 2, we consider how to set up the harvesting threshold value h. We find that h_1 is an important harvesting amount. If the harvesting threshold value exceeds h_1, the system does not have a positive equilibrium; that is, the predator eventually tends to extinction. If the harvesting threshold value is less than h_1, the system has two positive equilibria among which one is unstable and the other may be stable, *i.e.*, the predator and prey may coexist.

Example 3.3. For model Equation (3), we choose $r = 0.1, K = 0.25, a = 0.25, c = 0.8, d = 0.01$, $m = 0.03$ and $P_0 = 0.1$. Thus we obtain $\hat{n} = 1.25$, $h_1 = 0.0032$, $h_2 = 0.0024$, and $\hat{P} = 0.16$. A bifurcation diagram is illustrated in Figure 3, where the horizontal blue line presents the curve of the predator with the positive equilibrium E^*. It displays that there is a bifurcation at $h = h_1$ when the parameter h reduces, which produces three equilibria E^* ,E_1 and E_2.

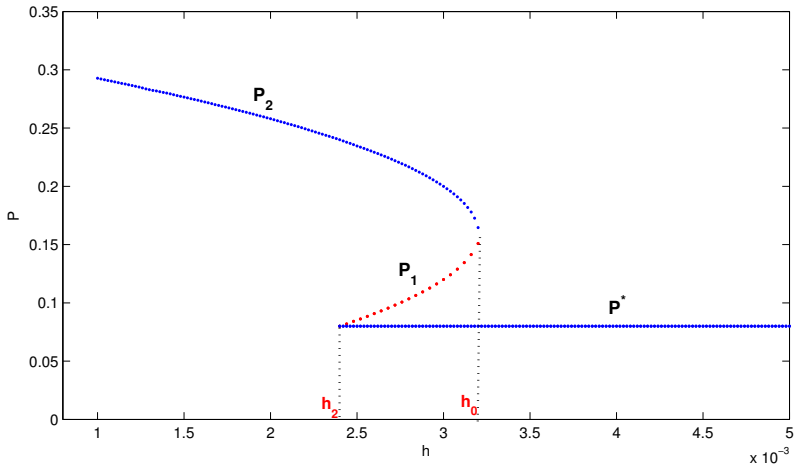

Figure 3. The bifurcation diagram with P_1, P_2 and P^* *versus* h. The lines with P_1 and P_2 indicate the curves of the predator with coexistent equilibria E_1 and E_2, respectively, and the line with P^* indicates the curve of the predator with coexistent equilibrium E^*.

The existence of limit cycles plays an important role in determining the dynamical behavior of the system. For example, if there is no limit cycle in system Equation (3) and its positive equilibrium is unique and locally asymptotically stable, then it must be globally stable. Now, we explore the existence of limit cycles in system Equation (3).

Theorem 7. *Suppose $\hat{n} > 1$ and $h < min\{h_1, h_2\}$. If $\varphi > 0$, then system Equation (3) has at least a stable limit cycle which encircles E_1.*

Proof. For $\hat{n} > 1$ and $h < h_2$, it is known from Theorem 2 *a*) that the equilibrium E^* of system Equation (3) does not exist. Furthermore, because $\hat{n} > 1$, $h < h_1$, and $h < h_2$, it follows from Theorem 2 *b*) that the equilibrium E_2 of system Equation (3) does not exist, but the equilibrium E_1 exists.

It follows from $\varphi > 0$ that E_1 is an unstable focus or node. It is easy to see that the unstable manifold at the saddle point $E_0(K, 0)$ is in the first quadrant. As the set D is positively invariant for system Equation (3), and system Equation (3) does not have any equilibrium in the interior of $D \setminus \{E_1\}$. It follows from the Poincaré-Bendixson theorem that system Equation (3) has at least a stable limit cycle which encircles E_1. □

In general, Dulac functions are only applied to smooth vector fields in the study of nonexistence of limit cycles. Since the right-hand sides of Equation (3), denoted by f_1 and f_2, are not smooth, following the similar arguments as in Wang ([31] Lemma 3.2), which is based on *Green's* Theorem, we are able to obtain sufficient conditions for the nonexistence of limit cycles in system Equation (3).

Theorem 8. *System Equation (3) does not have a limit cycle if $caK < d + r$.*

Proof. By the first equation of Equation (3), it is easy to see that the positive solutions of Equation (3) eventually enter and remain in the region

$$C = \{(N, P) : N \leq K\}$$

Thus, if a limit cycle exists, it must lie in the region C. Take a Dulac function $F = \frac{1}{N}$. Then we have

$$\frac{\partial(Ff_1)}{\partial N} + \frac{\partial(Ff_2)}{\partial P} = -\frac{r}{K} + ca - \frac{d+m}{N} \leq ca - \frac{d+m+r}{K} < 0$$

if $0 < P < P_0$. If $P > P_0$, it is easy to see that

$$\frac{\partial(Ff_1)}{\partial N} + \frac{\partial(Ff_2)}{\partial P} = -\frac{r}{K} + ca - \frac{d}{N} \leq ca - \frac{d+r}{K} < 0$$

Hence, system Equation (3) does not have a limit cycle. □

4. Numerical Simulation

In this section, we present numerical examples for system Equation (3).

Example 4.1. (**Example 3.1.** continued) The parameters values r, K, a, c, d and m are the same as in Example 3.1. We obtain $\hat{n} > 1$, $h_1 = 0.0081$, and $h_2 = 0.0072$. A forward bifurcation diagram is given in Figure 1.

Selecting $P_0 = 0.25$, we get $h = 0.0075 > h_2$. The equilibrium $E^*(0.2, 0.24)$ exists, but E_1 and E_2 do not exist (Theorem 2 *b*)). Its phase portrait is given in Figure 4, which shows that the unique positive equilibrium E^* is globally asymptotically stable.

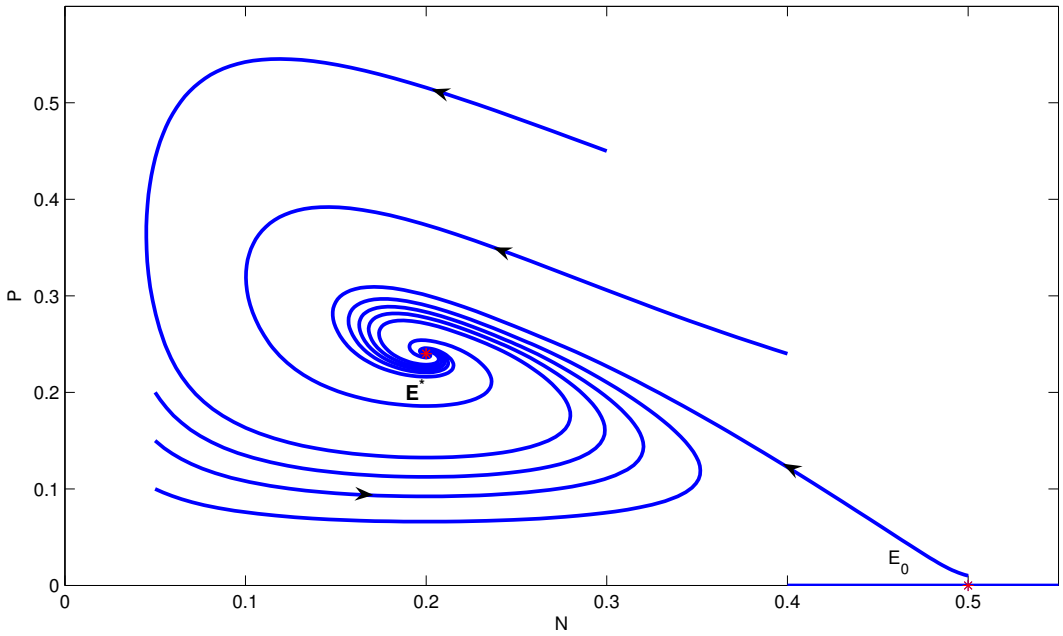

Figure 4. The phase portrait of model Equation (3) when E^* is globally asymptotically stable and E_0 is unstable.

If we choose $P_0 = 0.2$, then $h = 0.006 < h_2$. Equilibrium $E_1(0.16044, 0.27165)$ exists, but E_2 and E^* do not exist (Theorem 2 b)). Its phase portrait is given in Figure 5. The unique positive equilibrium E_1 is globally asymptotically stable in D.

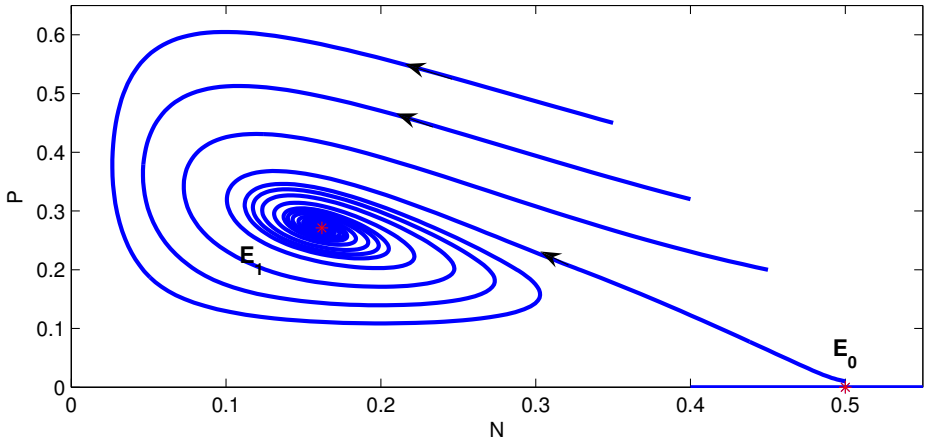

Figure 5. The phase portrait of model Equation (3) when E_1 is locally asymptotically stable and E_0 is unstable.

The equilibrium E^* in Figure 4 corresponds to some point on the curve of P^* in Figure 1 ($h > h_2$), and the equilibrium E_1 in Figure 5 corresponds to some point on the curve of P_1 in Figure 1 ($h < h_2$).

Example 4.2. (**Example 3.2.** continued) Choosing the same parameters values as in Example 3.2, we have $h_1 = 0.00378$ and $\hat{P} = 0.34367$. A backward bifurcation diagram is given in Figure 2.

If we choose $P_0 = 0.1$, then $P_0 < \hat{P}$. Equilibria $E_1(0.2, 0.5)$ and $E_2(0.325, 0.1875)$ exist, but equilibrium E^* does not exist. Its phase portrait is illustrated in Figure 6. It shows that equilibria E_0 and E_1 are asymptotically stable.

The equilibria E_1 and E_2 in Figure 6 correspond to some points on the curves of P_1 and P_2 , respectively, in Figure 2 ($h < h_1$).

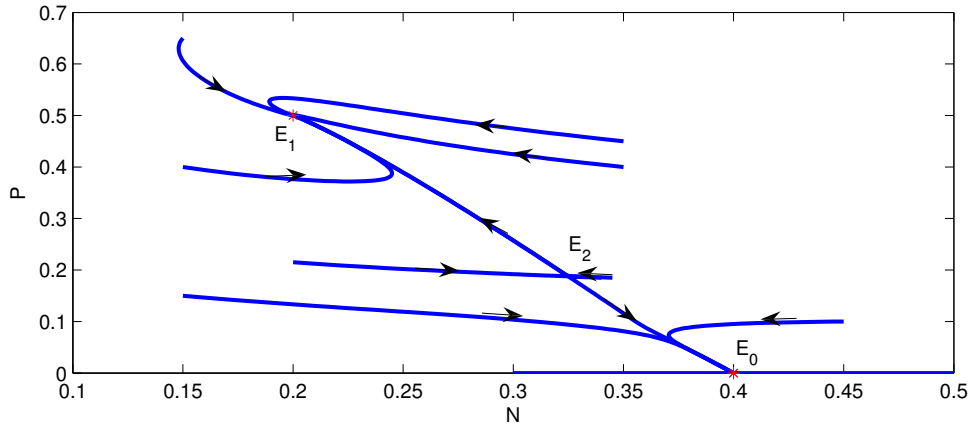

Figure 6. The phase portrait of model Equation (3) when E_0 and E_1 are locally asymptotically stable and E_2 is unstable.

Example 4.3 (I). (**Example 3.3.** continued) We identically select parameter values as in Example 3.3, and set $P_0 = 0.1$. Thus we have $\hat{n} > 1$, $h_1 = 0.0032$, $h_2 = 0.0024$, $\hat{P} = 0.16$, and $h = 0.003$. The above parameter values satisfy conditions $a)$ and $c)$ in Theorem 2, and condition $a)$ in Theorem 6.

Obviously, equilibria $E_0(0.25, 0)$, $E^*(0.2, 0.08)$, $E_1(0.125, 0.2)$, and $E_2(0.175, 0.12)$ all exist. The phase portrait of model Equation (3) is shown in Figure 7. Equilibria E^* and E_1 are asymptotically stable, and E_0 and E_2 are unstable. So model Equation (3) has bistable positive equilibria E^* and E_1.

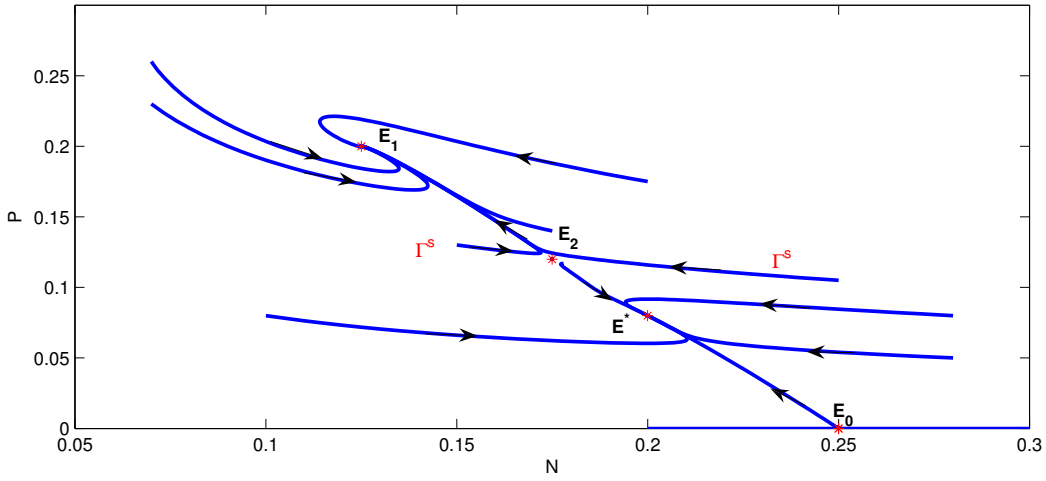

Figure 7. The phase portrait of model Equation (3) with bistable positive equilibria E^* and E_1, and unstable equilibria E_0 and E_2.

It follows from Figure 7 that the stable region Γ^s of the saddle point E_2 divides the positive invariant set into two regions. The attractive basin for the stable equilibrium E_1 is the region above Γ^s and the region below Γ^s is the basin of attraction for the stable equilibrium E^*.

The equilibria E_1 and E_2 in Figure 7 correspond to some points on the curves of P_1 and P_2, respectively, and E^* corresponds to some point on the curve of P^* in Figure 3 ($h_2 < h < h_1$).

Example 4.3 (II). We set parameter values $r = 0.03, K = 0.25, a = 0.5, c = 0.4, d = 0.01, m = 0.03$, and $P_0 = 0.0133$. Thus we have $\hat{n} = 1.25$, $uh_1 = 0.00048$, $h_2 = 0.00036$, $\hat{P} = 0.024$, and $h = 0.000399$. These parameter values satisfy conditions $a)$ and $c)$ in Theorem 2 and the condition $c)$ in Theorem 6. Thus, equilibria $E_0(0.25, 0)$, $E^*(0.2, 0.012)$, $E_1(0.1092, 0.0338)$, and $E_2(0.1908, 0.0142)$ all exist. The phase portrait of model Equation (3) is shown in Figure 8. Equilibria E^* and E_1 are stable, and E_0 and E_2 are unstable. So model Equation (3) has bistable positive equilibria E^* and E_1.

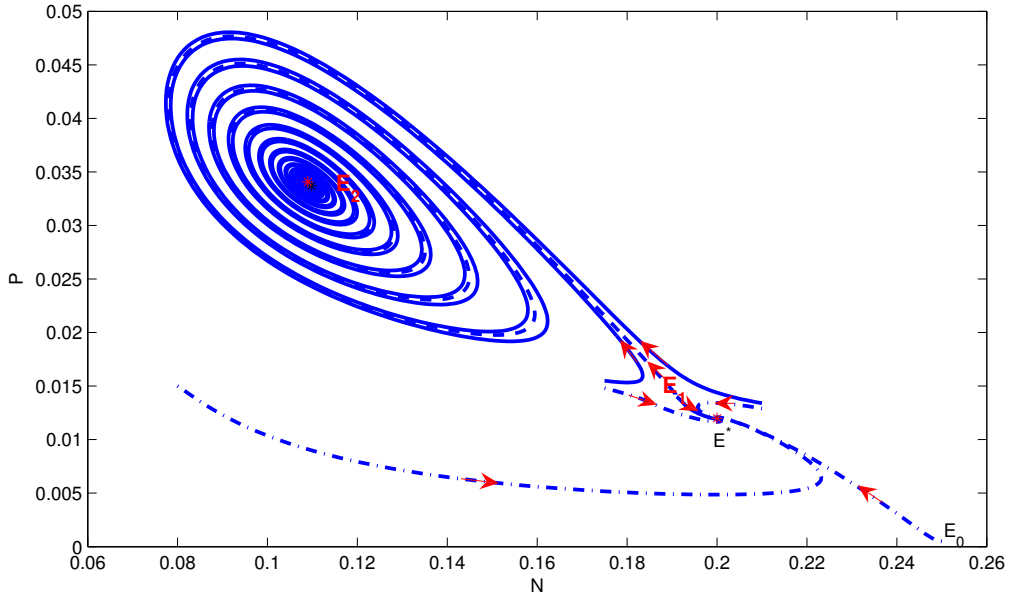

Figure 8. The phase portrait of model Equation (3) with positive stable equilibria E^* and E_1, and unstable equilibria E_0 and E_2.

The model with the parameter values in Example 4.3 (II) has a similar bifurcation diagram as that in Example 4.3 (I), and the stability of equilibria in Figure 8 is identical with that in Figure 7.

Example 4.4 (I). We select $r = 0.004, K = 0.2, a = 0.1, c = 0.4, d = 0.001$ and $m = 0.005$. Then $\hat{n} = 1.333$, $h_1 = 6.125 * 10^{-5}$, $\hat{P} = 1.75 * 10^{-2}$, and $h_2 = 5 * 10^{-5}$.

Choosing $P_0 = 0.008$, we have $h = 2 * 10^{-5}$. Thus, $h < h_2 < h_1$, $P_0 < \hat{P}$, $caK > r$, $h > h_3$, and $\eta < 0$. Equilibrium $E_1(0.04069, 0.03186)$ exists but is unstable, and E^* and E_2 do not exist. The parameter values satisfy the conditions of Theorem 7. Its phase portrait is given in Figure 9, which shows that model Equation (3) has a stable limit cycle which encircles E_1.

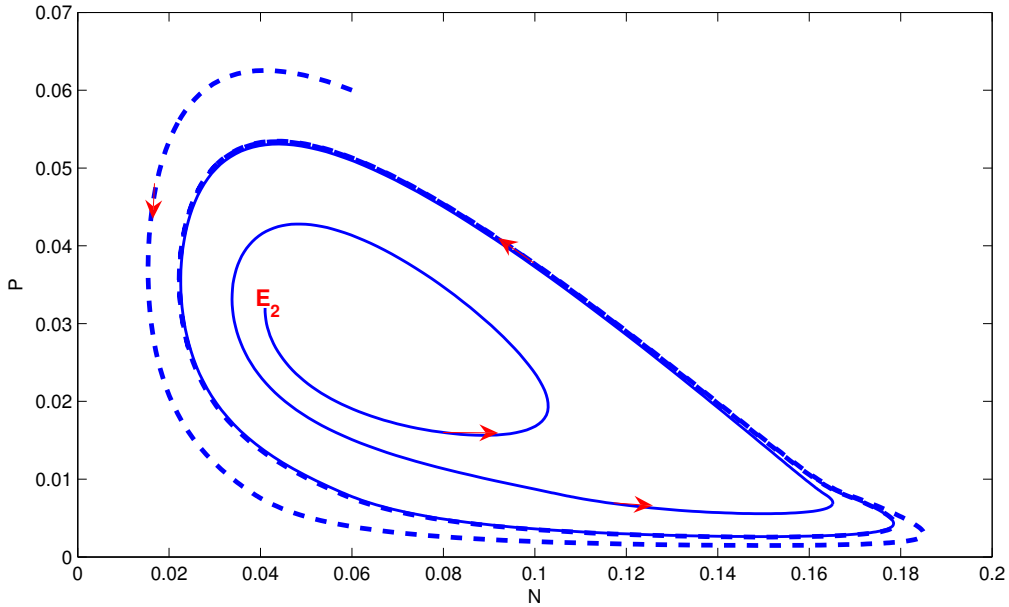

Figure 9. A stable limit cycle of model Equation (3) encircling the unstable equilibrium E_1.

Example 4.4 (II). Set $r = 0.03, K = 0.264, a = 0.5, c = 0.4, d = 0.01$, and $m = 0.031$. We obtain $\hat{n} = 1.2878$, $h_1 = 5.2041 * 10^{-4}$, $\hat{P} = 2.4318 * 10^{-2}$, and $h_2 = 4.1568 * 10^{-4}$.

Choosing $P_0 = 0.0133$, we obtain $h = 4.123 * 10^{-4}$. The parameter values satisfy Theorem 2 (b) and Theorem 6 (c), but do not satisfy Theorem 2 (a). Thus, equilibria E^* and E_2 do not exist and $E_1(0.1082, 0.0354)$ exists. The phase portrait of model Equation (3) is shown in Figure 10. In Figure 10, equilibrium E_1 is stable and two periodic orbits encircle E_1. We can see that the outside periodic orbit is stable. However, the inside periodic orbit is unstable. A trajectory (the dotted line) between the outside and inside periodic orbits ultimately tends to the outside periodic orbit, but a trajectory (the thin black line) starting from within the unstable periodic orbit finally tends to equilibrium E_1. So the initial state is important for ultimate trends of trajectories.

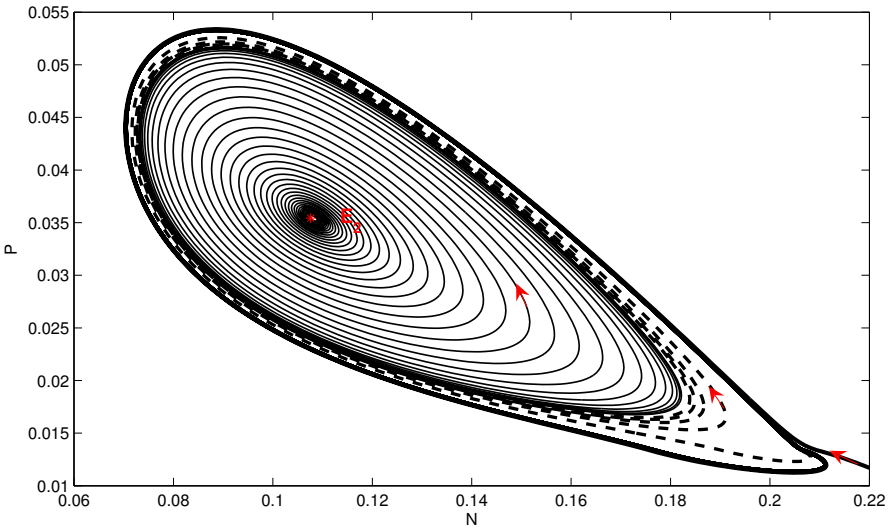

Figure 10. The phase portrait of model Equation (3) when E_1 is stable.

5. Conclusions

In this paper, we proposed and studied a new predator-prey model with non-smooth switched harvest on the predator. If the density of the predator is below a switched value, the harvest has a linear harvesting rate. Otherwise, the harvesting rate is constant. Our model exhibits new dynamical features compared to those with a linear harvesting rate or a constant harvesting rate.

According to the Kolmogorov Theorem [38], under certain assumptions, the model with a linear predator harvesting rate has either a stable equilibrium or a stable limit cycle, whereas the model with a constant harvesting rate on the predator has richer dynamics [16,23,23]. For example, for a class of predator-prey systems, Brauer and Soudack [23,23] obtained different types of dynamics for which the harvesting was in prey or a predator; Xiao and Jennings [16] further studied a ratio-dependent predator-prey model with a constant harvest on prey. They proved that the model could exhibit complicated bifurcation phenomena, including the Bogdanov-Takens bifurcation of cusp type, the heteroclinic bifurcation, or a separatrix connecting a saddle-node and a saddle bifurcation.

For the model studied in this paper, we showed that (see Theorem 2 and Corollary 1) a backward bifurcation from the predator-prey coexistence equilibrium may occur, which shows that reducing the net reproductive number of the predator to less than unity is not enough to eradicate the predator. On the other hand, when the net reproductive number of the predator is greater than unity, we showed that the predator always coexists with the prey permanently (Theorem 3), and the model may exhibit the following dynamics: (i) a unique globally asymptotically stable coexistence equilibrium; (ii) the coexistence of positive saddle equilibria connecting with either a locally asymptotically stable positive equilibrium (biostable) or a limit cycle; (iii) two stable positive equilibria coexisting with a saddle point. By numerical examples, we also showed that the model

could exhibit more new dynamical features: (a) a limit cycle encircling a unique positive equilibrium (see Figure 9); (b) two cycles surround an identical positive equilibrium, with one stable and one unstable (see Figure 10).

We would like to point out that we have assumed the simple functional response of the bilinear type in our current model Equation (3). We may also consider other types of functional responses. The dynamics may be richer and more complex. Further investigations are planned in our future studies.

Acknowledgments: Bing Li is supported by Natural Science Foundation of Heilongjiang A201411. Shengqiang Liu is supported by the NNSF of China (No. 11471089, 11301453) and the Fundamental Research Funds for the Central Universities (No.HIT.IBRSEM.A.201401). Jing'an Cui is supported by the National Natural Science Foundation of China (11371048, 11071011) and Funding Project for Academic Human Resources Development in Institutions of Higher Learning Under the Jurisdiction of Beijing Municipality(PHR201107123). Jia Li is supported partially by U.S. National Science Foundation grant DMS-1118150.

Author Contributions: Jia Li and Shengqiang Liu conceived and designed the study; Bing Li performed the simulation; Jing'an Cui participated in the analysis of the results; Bing Li, Jia Li and Shengqiang Liu wrote the paper. All authors read and approved the manuscript.

Conflicts of Interest: The authors declare no conflict of interest.

References

1. Murdoch, W.W.; Briggs, C.J.; Nisbet, R.M. *Consumer-Resource Dynamics*; Princeton University Press: Princeton, NJ, USA, 2003.
2. Seo, G.; DeAngelis, D.L. A predator-prey model with a Holling type I functional response including a predator mutual interference. *J. Nonlinear Sci.* **2011**, *21*, 811–833.
3. Turchin, P. *Complex Population Dynamics: A Theoretical/empirical Synthesis*; Princeton University Press: Princeton, NJ, USA, 2003.
4. Gutierrez, A.P. *Applied Population Ecology: A Supply-Demand Approach*; John Wiley and Sons: New York, NY, USA, 1996.
5. Seo, G.; Kot, M. A comparison of two predator-prey models with Hollingąŕs type I functional response. *Math. Biosci.* **2008**, *212*, 161–179.
6. Cushing, J.M.; Zou, Y. The net reproductive value and stability in matrix population models. *Nat. Resour. Model.* **1994**, *8*, 297–333.
7. Cushing, J.M. *An Introduction to Structured Population Dynamics*; SIAM: Philadelphia, PA, USA, 1998.
8. Kar, T.K. Stability analysis of a prey-predator model incorporating a prey refuge. *Commun. Nonlinear Sci. Numer. Simul.* **2005**, *10*, 681–691.
9. Chakraborty, K.; Haldar, S.; Kar, T.K. Global stability and bifurcation analysis of a delay induced prey-predator system with stage structure. *Nonlinear Dyn.* **2013**, *73*, 1307–1325.
10. Liu, S.Q.; Beretta, E. A stage-structured predator-prey model of Beddington-Deangelis type. *SIAM J. Appl. Math.* **2006**, *66*, 1101–1129.
11. Qu, Y.; Wei, J.J. Bifurcation analysis in a time-delay model for preyÍCpredator growth with stage-structure. *Nonlinear Dyn.* **2007**, *49*, 285–294.
12. Zhang, X.A.; Chen, L.S.; Neumann, A.U. The stage-structured predator-prey model and optimal harvesting policy. *Math. Biosci.* **2000**, *168*, 201–210.
13. Zhang, Y.; Zhang, Q.L. Dynamic behavior in a delayed stage-structured population model with stochastic fluctuation and harvesting. *Nonlinear Dyn.* **2011**, *66*, 231–245.
14. Lai, X.H.; Liu, S.Q.; Lin, R.Z. Rich dynamical behaviours for predator-prey model with weak Allee effect. *Appl. Anal.* **2010**, *89*, 1271–1292.
15. Lin, R.Z.; Liu, S.Q.; Lai, X.H. Bifurcations of a predator-prey system with weak Allee effects. *J. Korean Math. Soc.* **2013**, *50*, 695–713.
16. Xiao, D.M.; Jennings, L.S. Bifurcations of a ratio-dependent predator-prey system with constant rate harvesting. *SIAM J. Appl. Math.* **2005**, *65*, 737–753.
17. Xiao, D.M.; Li, W.X.; Han, M.A. Dynamics in a ratio-dependent predator-prey model with predator harvesting. *J. Math. Anal. Appl.* **2006**, *324*, 14–29.

18. Zhang, Y.; Zhang, Q.L.; Zhang, X. Dynamical behavior of a class of prey-predator system with impulsive state feedback control and Beddington-DeAngelis functional response. *Nonlinear Dyn.* **2012**, *70*, 1511–1522.
19. Gao, Y.; Liu, S.Q. Global stability for a predator-prey model with dispersal among patches. *Abstr. Appl. Anal.* **2014**, *2014*, 176493.
20. Martin, A.; Ruan, S.G. Predator-prey models with delay and prey harvesting. *J. Math. Biol.* **2001**, *43*, 247–267.
21. Wei, C.J.; Chen, L.S. Periodic solution and heteroclinic bifurcation in a predatorÍCprey system with Allee effect and impulsive harvesting. *Nonlinear Dyn.* **2014**, *76*, 1109–1117.
22. Azar, C.; Holmberg, J.; Lindgren, K. Stability analysis of harvesting in a predator-prey model. *J. Theor. Biol.* **1995**, *174*, 13–19.
23. Brauer, F.; Soudack, A.C. Stability regions and transition phenomena for harvested predator-prey systems. *J. Math. Biol.* **1979**, *7*, 319–337.
24. Brauer, F.; Soudack, A.C. Stability regions in predator-prey systems with constant-rate prey harvesting. *J. Math. Biol.* **1979**, *8*, 55–71.
25. Kar, T.K. Selective harvesting in a prey-predator fishery with time delay. *Math. Comput. Model.* **2003**, *38*, 449–458.
26. Lenzini, P.; Rebaza, J. Nonconstant predator harvesting on ratio-dependent predator-prey models. *Appl. Math. Sci.* **2010**, *4*, 791–803.
27. Negi, K.; Gakkhar, S. Dynamics in a Beddington-DeAngelis prey-predator system with impulsive harvesting. *Ecol. Model.* **2007**, *206*, 421–430.
28. Xiao, M.; Cao, J.D. Hopf bifurcation and non-hyperbolic equilibrium in a ratio-dependent predator-prey model with linear harvesting rate: Analysis and computation. *Math. Comput. Model.* **2009**, *50*, 360–379.
29. Beddington, J.R.; Cooke, J.K. Harvesting from a prey-predator complex. *Ecol. Model.* **1982**, *14*, 155–177.
30. Hu, Z.X.; Ma, W.B.; Ruan, S.G. Analysis of an SIR epidemic model with nonlinear incidence rate and treatment. *Math. Biosci.* **2012**, *238*, 12–20.
31. Wang, W.D. Backward bifurcation of an epidemic model with treatment. *Math. Biosci.* **2006**, *201*, 58–71.
32. Zhang, X.; Liu, X.N. Backward bifurcation and global dynamics of an SIS epidemic model with general incidence rate and treatment. *Nonlinear Anal. Real World Appl.* **2009**, *10*, 565–575.
33. Cantrell, R.S.; Cosner, C. On the dynamics of predator-prey models with the Beddington—DeAngelis functional response. *J. Math. Anal. Appl.* **2001**, *257*, 206–222.
34. Lu, Y.; Li, D.; Liu, S.Q. Modeling of hunting strategies of the predators in susceptible and infected prey. *Appl. Math. Comput.* **2016**, *284*, 268–285.
35. Hale, J.; Waltman, P. Persistence in infinite-dimensional systems. *SIAM J. Math. Anal.* **1989**, *20*, 388–395.
36. McCluskey, C. Lyapunov Functions for Tuberculosis Models with Fast and Slow Progression. *Math. Biol. Eng.* **2006**, *3*, 603–614.
37. Hale, J.; Lunel, S.V. *Introduction to Functional Differential Equations*; Springer-Verlag: New York, NY, USA, 1993.
38. Freedman, H.I. *Deterministic Mathematical Models in Population Ecology*; Marcel Dekker: New York, NY, USA, 1980.
39. Cui, J. ; Mu, X.; Wan, H. Saturation recovery leads to multiple endemic equilibria and backward bifurcation. *J. Theor. Biol.* **2008**, *254*, 275–283.
40. Van den Driessche, P.; Watmough, J. Reproduction numbers and sub-threshold endemic equilibria for compartmental models of disease transmission. *Math. Biosci.* **2002**, *180*, 29–48.
41. McQuaid, C.F.; Britton, N.F. Trophic structure, stability, and parasite persistence threshold in food webs. *Bull. Math. Biol.* **2013**, *75*, 2196–2207.
42. Zhang, X.; Liu, X.N. Backward bifurcation of an epidemic model with saturated treatment function. *J. Math. Anal. Appl.* **2008**, *348*, 433-443.
43. Zhou, L.H.; Fan, M. Dynamics of an SIR epidemic model with limited medical resources revisited. *Nonlinear Anal. Real World Appl.* **2012**, *13*, 312–324.